

Instabilities of localized structures in dissipative systems with delayed feedback

S. V. Gurevich* and R. Friedrich

Institute for Theoretical Physics,

University of Münster,

Wilhelm-Klemm-Str. 9,

D-48149 Münster, Germany

(Dated: December 3, 2024)

Abstract

We are interested in the stability of single localized structures in a real Swift-Hohenberg equation subjected to a delayed feedback. We shall show that variation in the product of the delay time and the feedback strength leads to complex dynamical behavior of the system, including formation of oscillons, soliton rings, labyrinth patterns or moving structures. We provide a bifurcation analysis of the delayed system and derive a system of order parameter equations for the position of the localized structure as well as for its shape. In a special case, a normal form of the delay-induced drift-bifurcation is obtained, showing that spontaneous motion to the lowest order arises without change shape.

PACS numbers: 02.30.Ks, 02.30.Oz, 05.45.Yv

Control and engineering of complex spatio-temporal patterns in high-dimensional non-equilibrium systems has evolved as one of the central issues in applied nonlinear science [1, 2]. A number of different control techniques have been developed within the last decade. Among other methods, a quite simple and efficient scheme is the time delayed feedback (TDF) [3] (also referred to as Pyragas control or time-delay autosynchronization). Although TDF method was originally designed to control dynamical systems with a few degrees of freedom, it has been successfully applied to a large number of theoretical and experimental high-dimensional spatially extended systems [4]. In particular, control of self-organized localized solitary patterns in dissipative systems have been of increasing interest in recent years. Dissipative localized structures (LSs) turned out to be of a particular interest for fundamental research as well as for applications (see, e.g. [5, 6] and references thereafter). In particular, traveling pulses and fronts subjected to a TDF appear in various contexts. We mention only propagating depolarization waves appearing for both migraine and stroke [7], spreading of biological species [8] and delay-induced motion of one-dimensional fronts in reaction-diffusion systems [9]. In nonlinear optics, a model for the study of LSs, referred to as cavity solitons (CSs), in board area vertical-cavity surface-emitted lasers subjected to TDF was proposed in [10]. Recently, properties of two-dimensional CSs by means of a real Swift-Hohenberg equation subjected to TDF were studied in [11]. It was shown that when the product of the delay time and the feedback strength exceeds some critical value, single CS starts to move in an arbitrary direction. Moreover, an analytical formula for its velocity was derived. We refer to such kind of instability as *delay-induced drift-bifurcation*.

In this Letter we investigate the stability of a single LS in a real Swift-Hohenberg equation subjected to a TDF in details. Varying of the product of the delay time and the feedback strength, among moving LSs, also leads to the formation of complex spatio-temporal patterns, such as oscillons, soliton rings or labyrinths. Moreover, we provide a bifurcation analysis of the delayed system and derive a set of order parameter equations for the position of the CS as well as for its shape. In a special case, a normal form of the delay-induced drift-bifurcation is also derived, showing that the drift-induced motion can arise without pronounced change of the LS's shape. The bifurcation analysis is performed in general form and therefore can be applied to any system possessing solutions in form of LSs.

We start with the delayed Swift-Hohenberg equation (DSHE) [11]

$$\frac{\partial X}{\partial t} = -a_1 \nabla^2 X - a_2 \nabla^4 X + f(X) + \alpha (X(t) - X(t - \tau)), \quad (1)$$

where $X := X(\mathbf{x}, t)$, $\mathbf{x} = (x, y)^T$ is the real distributed order parameter, describing the deviation of the cavity field, $a_1, a_2 > 0$, τ is the delay time, whereas α denotes the positive delay strength. In the polynomial nonlinear function $f(X) = Y + C X - X^3$ the coefficient Y describes the deviation of the injection field and C is the cooperative parameter. The derivation of the Eq. (1) as well as detailed description of physical meaning of the parameters can be found in [11, 12]. Without the TDF, i.e., for $\alpha = 0$ Eq. (1) becomes the Swift-Hohenberg equation (SHE), describing nascent optical bistability in the weak dispersion limit [13]. An important property of SHE is its variational structure, i.e., it possesses a Lyapunov functional. This means that no Hopf bifurcations as well as time-dependent solutions are possible. Furthermore, stable stationary LSs are homoclinic solutions of SHE with $\partial X / \partial t = 0$. Notice that in the presence of TDF Eq. (1) loses the gradient structure. Nevertheless the homogeneous steady states as well as stationary localized solutions are not affected by the TDF. However, their stability properties may change.

In order to investigate the stability of the stationary solutions as well as of the homogeneous steady states we rewrite the evolution equation Eq. (1) in the general form

$$\partial_t \mathbf{q}(\mathbf{x}, t) = \mathfrak{L} \mathbf{q}(\mathbf{x}, t) + \alpha \mathbf{E} (\mathbf{q}(\mathbf{x}, t) - \mathbf{q}(\mathbf{x}, t - \tau)). \quad (2)$$

Here, \mathfrak{L} denotes the nonlinear Swift-Hohenberg operator and \mathbf{E} is the identity matrix. Notice that the function $X(\mathbf{x}, t)$, given by Eq. (1) is a scalar quantity. Nevertheless for the sake of generality Eq. (2) is written in terms of a vector function $\mathbf{q} = \mathbf{q}(\mathbf{x}, t)$, $\mathbf{x} = (x, y)^T$. We assume that the stationary solution of (2) $\mathbf{q}_0 := \mathbf{q}_0(\mathbf{x})$ exists. In the simplest case it is a single stationary LS with rotational symmetry. It exists for all values of the delay strength α and is determined by the condition $\mathfrak{L} \mathbf{q}_0 = 0$. For $\alpha = 0$ linear stability analysis of \mathbf{q}_0 yields a real spectrum, given by the linear eigenvalue problem of the form $\mathfrak{L}'(\mathbf{q}_0) \boldsymbol{\varphi} = \mu \boldsymbol{\varphi}$, since the linearization operator $\mathfrak{L}'(\mathbf{q}_0)$ is self-adjoint. Note that due to translational invariance $\mu = 0$ is an eigenvalue of $\mathfrak{L}'(\mathbf{q}_0)$, corresponding to two independent neutral eigenfunctions $\boldsymbol{\varphi}_{\mathbf{x}}^{\mathcal{G}}$, also referred to as Goldstone modes, which can be obtained as derivative of \mathbf{q}_0 with respect to spatial coordinates. The discrete spectrum of $\mathfrak{L}'(\mathbf{q}_0)$ in two dimensions turns out to contain modes $\propto \boldsymbol{\varphi}_n(\mathbf{x}) e^{in\phi}$ with $n = 0, \pm 2$. Here, the mode with $n = 0$ results in the

change of the size of the LS, and $n = \pm 2$ lead to deformation of the LS. All other modes are strongly damped. We suppose that in the absence of the TDF the stationary solution \mathbf{q}_0 is stable, i.e., all eigenvalues but $\mu = 0$ have negative real parts.

For $\alpha \neq 0$ the spectrum of the corresponding linear operator can be constructed from the spectrum of $\mathcal{L}'(\mathbf{q}_0)$, since the latter commutes with the identity coupling matrix. Indeed, both operators possess the same set of eigenfunctions $\boldsymbol{\varphi}(\mathbf{x})$, whereas the complex eigenvalues λ of the delayed problem are determined as solutions of the transcendental equation [11]:

$$\mu = \lambda - \alpha (1 - e^{-\lambda\tau}), \quad (3)$$

that can be found in terms of Lambert W-functions [14] as

$$\lambda = \mu + \alpha + \frac{1}{\tau} W_m(-\alpha\tau \exp(-(\mu + \alpha)\tau)), \quad m \in \mathbb{Z}.$$

That is, the stationary solution of (2) remains stable, if $\text{Re}(\lambda(\mu)) < 0$ for any μ from the spectrum of $\mathcal{L}'(\mathbf{q}_0)$. Bifurcation points correspond to μ , at which $\text{Re}(\lambda(\mu))$ vanishes. In particular, instability criterion for all eigenvalues λ , corresponding to the real eigenvalues μ from the discrete spectrum of $\mathcal{L}'(\mathbf{q}_0)$, is given by the relation $a := \alpha\tau \geq \max\{-\mu\tau/2, 1\}$. One can see that $\mu = 0$ yields the bifurcation point $a = 1$, corresponding to the onset of delay-induced spontaneous motion, observed in [11]. Furthermore, eigenvalues μ of discrete critical modes $n = 0, n = \pm 2$ of the operator $\mathcal{L}'(\mathbf{q}_0)$ are close to zero, that is, for typical system parameters the instability threshold yields the value $a = 1$, which becomes the bifurcation point of higher codimension. In addition, using a as a control parameter, one can find a critical delay time $\tau_c := x a / \mu$ for which each of the critical modes becomes unstable by means of the following solvability condition:

$$\pm \arccos(1 + x) + 2\pi m = \pm a \sqrt{1 - (1 + x)^2}, \quad m \in \mathbb{Z}. \quad (4)$$

The next point to emphasize is that the TDF can also affect the stability of the homogeneous solution \mathbf{q}_h of the system (2) [12]. Indeed, for $\alpha = 0$ the linear stability of the homogeneous solution is given by the dispersion relation $\mu(k) = a_1 k^2 - a_2 k^4 + f'(\mathbf{q}_h)$. As before let us suppose that in the absence of the TDF the homogeneous solution is stable, that is, $\mu(k) < 0$ for all values of k . For $\alpha > 0$ the linear stability analysis with respect to perturbations in the form $\propto \exp(i k \mathbf{x} + \lambda(k)t)$ leads us to the same transcendental equation (3), where both μ and λ become functions of the wave vector k . As noted above, the solutions of this equation can

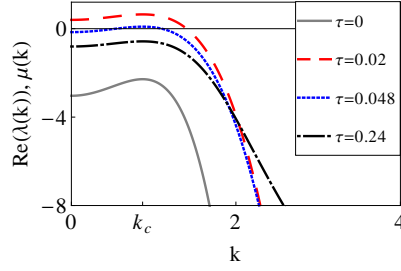


Figure 1. A real part of the dispersion function $\lambda(k)$, calculated at $a = 1.05$ for three different values of the delay time τ , corresponding to a homogeneous Hopf bifurcation with $k = 0$ for $\tau = 0.02$ (dashed red line), a traveling wave bifurcation with $k = k_c$ for $\tau = 0.048$ (dotted blue line) as well as stable homogeneous solution \mathbf{q}_h for $\tau = 0.24$ (black dash-dotted line). Only the main branch of $\text{Re}(\lambda(k))$ is shown. A gray solid line corresponds to the dispersion function $\mu(k)$ for $\tau = 0$.

be found in the form of Lambert W-functions, and depend on both control parameters a and τ . The dependence of $\text{Re}(\lambda(k))$ on the delay time τ , calculated for fixed value of $a = 1.05$ is presented in Fig. 1. Only the main branch of the solution, corresponding to the function W_0 is shown as other branches are situated far away from zero for rather small values of a and τ . One can see that for $\tau = 0$ the homogeneous solution is stable. However, for $\tau > 0$ the behavior of the real part of $\lambda(k)$ indicates the existence of a pair of homogeneous Hopf bifurcations (HH) with $k = 0$ (see Fig. 1 for $\tau = 0.02$) as well as traveling wave bifurcations (TW) with a finite wave number $k = k_c$ (Fig. 1 for $\tau = 0.048$) [12]. The thresholds, associated with these instabilities can be found within the same solvability condition (4) as for the stability analysis of \mathbf{q}_0 . Further increasing of τ leads to the stabilization of the homogeneous solution \mathbf{q}_h (Fig. 1 for $\tau = 0.24$). Here $\text{Re}(\lambda(k))$ vanishes at $k = k_c = \pm\sqrt{a_1/2a_2}$, which is the most unstable wave number even in the absence of the delay. Notice that the behavior of $\text{Re}(\lambda(k))$ for large k is different for different values of τ . While for small values of τ the real part of $\lambda(k)$ decays as k^4 for large k , it decays rather as k^2 for larger values of the delay time, which is more in the nature of e.g., reaction-diffusion systems. Hence, in this parameter region one would expect a non-trivial spatial-temporal dynamics that is not generic for the solutions of the SHE.

In Fig. 2 a bifurcation diagram in (a, τ) plane, summarizing results, obtained from a linear stability analysis of both solutions \mathbf{q}_0 and \mathbf{q}_h is presented. Each line on the plot is a solution of the solvability condition (4), calculated for different values of control parameter a and

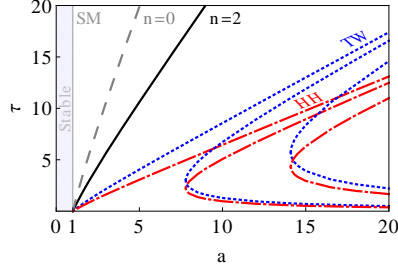


Figure 2. Bifurcation diagram in (a, τ) plane. Different lines separate instability regions, corresponding to different modes $n = 0$ (dashed gray line), $n = 2$ (solid black line), which are responsible for the instability of the stationary solution \mathbf{q}_0 as well as instability thresholds of traveling wave (TW) bifurcation (dotted blue curves) and Hopf (HH) bifurcation (dashed-dotted red curves) of the homogeneous solution \mathbf{q}_h . The vertical line at $a = 1$ indicated the onset of spontaneous motion (SM).

represents the instability thresholds for critical modes which are responsible for the stability properties of the stationary solution as well as thresholds for HH and TW bifurcations of the homogeneous solution. One can see that for $a < 1$ both solutions \mathbf{q}_0 and \mathbf{q}_h are stable. For $a = 1$ all modes become unstable simultaneously. However, for $a > 1$ the instability type depends on the value of the delay time τ . This is illustrated in Fig. 3, where results of direct numerical simulations of Eq. (1) for $a = 1.05$ and different values of τ are shown. Obviously for small values of τ all modes are excited. That is, one expects a complex dynamical behavior of the LS in this region. This case is illustrated in Fig. 3 for $\tau = 0.04$. After a few time steps an initial condition in form of a stationary LS with positive amplitude (a bright CS) becomes unstable and transforms into a stable breathing LS with negative amplitude (a dark CS). Here, the homogeneous steady state transfers to a new oscillatory state of a high positive amplitude, i.e., a transition from the bright CS to a dark oscillon is observed. If τ is increased, homogeneous solution becomes stable, but the spatial modes remain unstable and a soliton ring (see Fig. 3 for $\tau = 0.16$) or a labyrinth pattern ($\tau = 0.24$) is formed. In fact, in this parameter region all critical modes are unstable, i.e., the LS starts to move with a rather large velocity, its shape changes ($n = 0$) and deforms ($n = 2$). The curvature instability impacts on the dynamics as well, what finally results in the formation of the labyrinth structure. It is worthy of note that labyrinth patterns are not solutions of the SHE without the TDF. However, as mentioned above, there exist parameter regions,

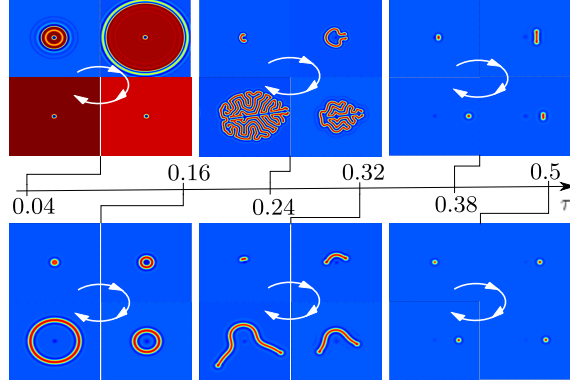


Figure 3. Numerical solutions of Eq. (1), obtained for fixed $a = 1.05$ and different values of the delay time τ . Numerical simulations have been performed on the two-dimensional square domain of the size 100×100 using a pseudo-spectral method with 512×512 grid points, whereas a Runge-Kutta 4 scheme is employed for the time stepping. Parameters are: $a_1 = -2$, $a_2 = -4/3$, $C = 1$, $Y = -0.4$. White arrows indicate the time evolution direction.

where the DSHE behaves like a reaction-diffusion system, where the formation of labyrinths is well understood [15]. This indicates that for certain values of the delay time the DSHE to some extent operates in the regime of reaction-diffusion systems. With increasing of τ the amplitudes of the unstable modes decrease, that is, instead of the labyrinths, a slowly moving wave segment emerges on the same time scale (see Fig. 3 for $\tau = 0.32$). Further increase in the delay time brings the system into the parameter region, where both modes $n = 0$ and $n = 2$ are stable, i.e., solutions in the form of moving LSs are expected. However, close to the instability threshold the real parts of corresponding eigenvalues are rather small, what affects the shape of the LS on a rather large time scale ($\tau = 0.38$). Finally, far away from the bifurcation point, the spontaneous motion with a constant velocity is observed as shown in Fig. 3 for $\tau = 0.5$. Notice, that in this case the dynamics of the LS is little affected by critical modes, that is, the CS propagates without pronounced change of its shape.

In order to investigate the stability of the localized structure as well as possible bifurcations in the presence of the delay term from the point of view of bifurcation theory we perform the following ansatz

$$\mathbf{q} = e^{-\mathbf{R}(t) \cdot \nabla} \left(\mathbf{q}_0(\mathbf{x}) + \mathbf{w}(\mathbf{x}, t) \right). \quad (5)$$

Here, the operator $e^{-\mathbf{R}(t) \cdot \nabla}$ generates a shift of the pattern to the spatial position $\mathbf{R}(t)$ and

$\mathbf{w}(\mathbf{x}, t) = \sum_j \varphi_j(\mathbf{x}) e^{\lambda_j t}$ is the shape deformation, given by a sum of all stable modes of the delayed problem. In the following, we shall decompose Eq. (2) in such a way, that an evolution equations for the shift $\mathbf{R}(t)$ as well as for the change of the shape of the LS in terms of the deformation $\mathbf{w}(\mathbf{x}, t)$ are derived. An equation for the shift $\mathbf{R}(t)$ can be obtained by requiring that the shape deformation is orthogonal to the Goldstone mode $\varphi_{\mathbf{x}}^{\mathcal{G}}$. This condition leads us to

$$\begin{aligned} -\dot{\mathbf{R}}(1 - \langle \varphi_{\mathbf{x}}^{\mathcal{G}} | \mathbf{w} \rangle) = & -\langle \varphi_{\mathbf{x}}^{\mathcal{G}} | \mathcal{L}'(\mathbf{q}_0) \mathbf{w} \rangle - \langle \varphi_{\mathbf{x}}^{\mathcal{G}} | \mathbf{N}(\mathbf{w}) \rangle \\ & -\alpha \langle \varphi_{\mathbf{x}}^{\mathcal{G}} | \mathbf{M}(\mathbf{x}, t, \mathbf{R}_t - \mathbf{R}_{t-\tau}, \mathbf{w}_t, \mathbf{w}_{t-\tau}) \rangle. \end{aligned} \quad (6)$$

Here, we introduce the nomenclature $\mathbf{R}_t := \mathbf{R}(t)$, $\mathbf{R}_{t-\tau} := \mathbf{R}(t - \tau)$, $\mathbf{w}_t := \mathbf{w}(\mathbf{x}, t)$ and $\mathbf{w}_{t-\tau} := \mathbf{w}(\mathbf{x}, t - \tau)$, the operator

$$\mathbf{N}(\mathbf{w}) = \frac{1}{2!} \mathcal{L}''(\mathbf{q}_0) \mathbf{w} : \mathbf{w} + \frac{1}{3!} \mathcal{L}'''(\mathbf{q}_0) \mathbf{w} : \mathbf{w} : \mathbf{w}$$

contains nonlinear contributions, whereas the delay terms are lumped into the operator

$$\begin{aligned} \mathbf{M} = & \mathbf{E} \left(1 - e^{(\mathbf{R}_t - \mathbf{R}_{t-\tau}) \cdot \nabla} \right) (\mathbf{q}_0(\mathbf{x}) + \mathbf{w}(\mathbf{x}, t)) \\ & + \mathbf{E} e^{(\mathbf{R}_t - \mathbf{R}_{t-\tau}) \cdot \nabla} (\mathbf{w}_t - \mathbf{w}_{t-\tau}) . \end{aligned}$$

The evolution equation for the shape deformation $\mathbf{w}(\mathbf{x}, t)$ is obtained by inserting the evolution equation (6) into Eq. (2):

$$\frac{\partial \mathbf{w}}{\partial t} = \tilde{\mathcal{L}}' \mathbf{w} + \dot{\mathbf{R}} \frac{\partial \mathbf{w}}{\partial \mathbf{x}} + \tilde{\mathbf{N}} + \alpha \tilde{\mathbf{M}}. \quad (7)$$

Here, the operator $\tilde{\mathcal{L}}' = \mathcal{L}' - \varphi_{\mathbf{x}}^{\mathcal{G}} \langle \varphi_{\mathbf{x}}^{\mathcal{G}} | \mathcal{L}' \rangle / \langle (\varphi_{\mathbf{x}}^{\mathcal{G}})^2 \rangle$ and other tilded operators $\tilde{\partial}/\partial \mathbf{x}$, $\tilde{\mathbf{N}}$, $\tilde{\mathbf{M}}$ are defined according to the same rule.

Equations (6) and (7) show that the deformation of the LS is given by a delayed equation and can be treated by a suitable bifurcation analysis. To this end, the form of the shape deformation should be specified. As we mentioned above, the critical modes of the operator $\mathcal{L}'(\mathbf{q}_0)$ are given by the discrete modes of the form $\varphi_0(\mathbf{x})$ and $\varphi_{\pm 2}(\mathbf{x}) e^{\pm i 2 \phi}$; all other modes are strongly damped. Therefore, as a first approximation, we can perform a mode truncation, representing the shape deformation $\mathbf{w}(\mathbf{x}, t)$ as a superposition of the modes of the discrete spectrum according to

$$\mathbf{w}(\mathbf{x}, t) = u_0(t) \varphi_0(\mathbf{x}) + u_2(t) \varphi_2(\mathbf{x}) e^{i 2 \phi} + c.c. ,$$

where the slow functions of time $u_0(t)$ and $u_2(t)$ are the amplitudes of modes $\varphi_0(\mathbf{x})$ and $\varphi_2(\mathbf{x})$, respectively. Projection of the evolution equation for the shape (7) onto these modes leads us to an ordinary set of delayed equations:

$$\begin{aligned}\dot{u}_0 &= \mu_0 u_0 + a_0 u_0^2 + b_0 |u_2|^2 + c_0 u_0^3 + d_0 u_0 |u_2|^2 \\ &\quad + \alpha(u_{0,t} - u_{0,t-\tau}), \\ \dot{u}_2 &= \mu_2 u_2 + b_2 u_0 u_2 + c_2 u_0^2 u_2 + d_2 |u_2|^2 u_2 \\ &\quad + \alpha(u_{2,t} - u_{2,t-\tau}).\end{aligned}\tag{8}$$

Here μ_0 and μ_2 are the eigenvalues of the operator $\mathcal{L}'(\mathbf{q}_0)$, corresponding to the modes $n = 0$, $n = 2$, respectively, and all coefficients are determined by the integrals $a_0 = \langle \varphi_0 | \mathcal{L}'' \varphi_0 \varphi_0 \rangle / 2$, $b_0 = \langle \varphi_0 | \mathcal{L}'' \varphi_2 \varphi_2 \rangle$, $c_0 = \langle \varphi_0 | \mathcal{L}''' \varphi_0 \varphi_0 \varphi_0 \rangle / 6$, $d_0 = \langle \varphi_0 | \mathcal{L}''' \varphi_0 \varphi_2 \varphi_2 \rangle$, $b_2 = \langle \varphi_2 | \mathcal{L}'' \varphi_0 \varphi_2 \rangle$, $c_2 = \langle \varphi_0 | \mathcal{L}''' \varphi_0 \varphi_0 \varphi_2 \rangle / 2$, $d_2 = \langle \varphi_2 | \mathcal{L}''' \varphi_2 \varphi_2 \varphi_2 \rangle / 2$. Furthermore, the delayed equation for the shift $\mathbf{R}(t)$ reads

$$\begin{aligned}\dot{\mathbf{R}} &= \alpha \left(1 - \sum_{k=0,\pm 2} D^k (u_{k,t} - u_{k,t-\tau}) \right) (\mathbf{R}_t - \mathbf{R}_{t-\tau}) \\ &\quad - \beta |\mathbf{R}_t - \mathbf{R}_{t-\tau}|^2 (\mathbf{R}_t - \mathbf{R}_{t-\tau}),\end{aligned}\tag{9}$$

with $\beta = \langle (\nabla \varphi_{\mathbf{x}}^{\mathcal{G}})^2 \rangle / \langle (\varphi_{\mathbf{x}}^{\mathcal{G}})^2 \rangle$. Thereby, the elements of the matrix D^k are defined as $D_{ij}^k = \langle \varphi_i^{\mathcal{G}} | \partial u_k(t) / \partial x_j \rangle$. A set of nonlinear delayed differential equations Eqs. (8)–(9) for the shape and the shift is a system of *order parameter equations*, describing the dynamical behavior of a single LS in the vicinity of the bifurcation point $a = 1$. Numerical solution of the system (8)–(9) gives us a time evolution of the amplitudes of the stable modes $u_0(t)$ and $u_2(t)$ as well as the evolution of the position $\mathbf{R}(t)$. In Fig. 4 (a) numerical solution of Eq. (8), showing relaxation oscillations of both critical modes is presented. Notice that simulation was performed in the parameter region, where a slow relaxation to the motion with a constant velocity (see Fig. 3 for $\tau = 0.38$) is observed.

The next point to emphasize is that Eqs. (8) admit solutions with $u_2 = 0$, i.e., solutions with rotationally symmetric structures, represented by interplay between the stable decaying breathing mode $n = 0$ and spontaneous motion. Solving the system (8)–(9) with $u_2 = 0$ numerically, an instability increment, calculated from the time evolution of the amplitude $u_0(t)$, can be calculated and compared with a decay rate, obtained from numerical simulations of Eq. (1) (see Fig. 4 (b)).

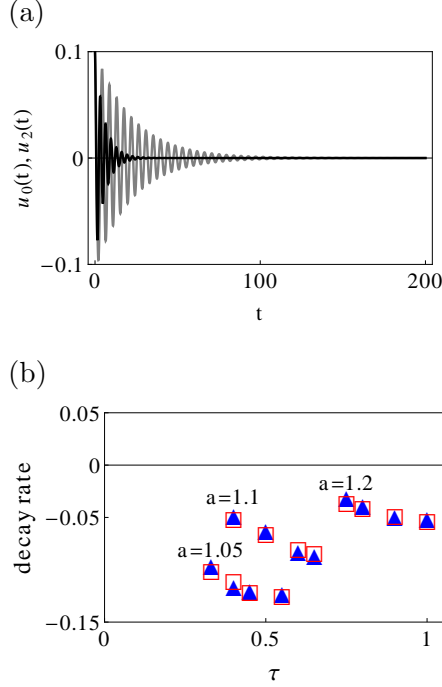


Figure 4. (a) Time evolution of the amplitudes $u_0(t)$ (gray) and $u_2(t)$ (black), as solutions of Eqs. (8), calculated for $\tau = 0.38$ and $a = 1.05$. Other parameters are the same as in Fig. 3. (b) Dependence of the instability increment on τ for three different values of the control parameter a as result of reduced model (8)-(9) (filled blue triangles) and direct numerical simulations of Eq. (1) (open red squares).

Now let us consider solutions with $u_0 = 0$, corresponding to the case of a spontaneous motion caused by the delay-induced drift-bifurcation. Let us define the drift velocity $\mathbf{V}(t) := \dot{\mathbf{R}}(t)$, which obeys Eq. (9). Since close to the bifurcation point $a = 1$, the velocity is slowly varying quantity in time we perform the approximation $\mathbf{R}(t - \tau) = \mathbf{R}(t) - \mathbf{V}(t)\tau + \tau^2\dot{\mathbf{V}}(t)/2 + \mathcal{O}(d^2\mathbf{V}/dt^2)$. The result is *the normal form* of the delay-induced drift-bifurcation

$$\begin{aligned} \dot{\mathbf{R}} &= \mathbf{V}, \\ \frac{a\tau}{2}\dot{\mathbf{V}} &= (a-1)\mathbf{V} - \frac{a}{6}\beta\mathbf{V}^2\mathbf{V}, \end{aligned} \quad (10)$$

which can be recognized as a normal form of the drift-bifurcation [6]. Notice that since $u_{0,2} = 0$, the delay-induced drift-bifurcation to the lowest order occurs *without change of shape* (compare to Fig. 3 for $\tau = 0.5$), what makes it different from the classical drift-

bifurcation [6]. The stationary drift velocity can be calculated directly from Eqs. (10),

$$V = \pm \frac{1}{\tau} \sqrt{\frac{6(a-1)}{\beta a}} \quad (11)$$

and to the lowest order is given by the same relation as calculated in [11].

To conclude we have shown that a SHE subjected to TDF exhibits complex spatio-temporal dynamics, including formation of, e.g. oscillons, soliton rings, labyrinth patterns or moving structures. The existence of labyrinth patterns indicates that in certain regions of the system parameters the DSHE to some extent behaves like a reaction-diffusion system. The mode truncation, neglecting contributions of the strongly damped modes of the continuous spectrum has led us to a system of order parameter equations, describing the behavior of the single LS in the DSHE. Moreover, in a special case, a normal form of the delay-induced drift-bifurcation is obtained, showing that induced motion to the lowest order can arise without change of the shape. In addition, presented analytical results are derived in general form and can be extended to other spatial extended systems.

We thank Dr. Andrei G. Vladimirov for fruitful discussions on the topic.

* gurevics@uni-muenster.de

- [1] A. S. Mikhailov and K. Showalter, Phys. Rep. **425**, 79 (2006)
- [2] *Handbook of Chaos Control*, 2nd ed., edited by E. Schöll and H. G. Schuster (Wiley, 2008)
- [3] K. Pyragas and A. Tamaševičius, Phys. Lett. A **180**, 99 (1993)
- [4] T. Pierre, G. Bonhomme, and A. Atipo, Phys. Rev. Lett. **76**, 2290 (1996) O. Lüthje, S. Wolff, and G. Pfister, *ibid.* **86**, 1745 (2001) N. Baba, A. Amann, E. Schöll, and W. Just, *ibid.* **89**, 074101 (2002) J. Schlesner, A. Amann, N. B. Janson, W. Just, and E. Schöll, Phys. Rev. E **68**, 066208 (2003) C. M. Postlethwaite and M. Silber, Physica D **236**, 65 (2007) Y. N. Kyrychko, K. B. Blyuss, S. J. Hogan, and E. Schöll, Chaos **19**, 043126 (2009)
- [5] *Dissipative Solitons: From Optics to Biology and Medicine*, edited by N. Akhmediev and A. Ankiewicz, Lecture Notes in Physics, Vol. 751 (Springer Berlin / Heidelberg, 2008)
- [6] H.-G. Purwins, H. U. Bödeker, and S. Amiranashvili, Adv. in Phys. **59**, 485 (2010)
- [7] M. A. Dahlem, F. M. Schneider, and E. Scholl, Chaos **18**, 026110 (2008) F. Schneider, E. Schöll,

- and M. Dahlem, *ibid.* **19**, 015110 (2009) M. A. Dahlem, R. Graf, A. J. Strong, J. P. Dreier, Y. A. Dahlem, M. Sieber, W. Hanke, K. Podoll, and E. Schöll, *Physica D* **239**, 889 (2010)
- [8] J. Fort and V. Méndez, *Phys. Rev. Lett.* **89**, 178101 (2002) V. Ortega-Cejas, J. Fort, and V. Méndez, *Ecology* **85**, 258 (2004)
- [9] T. Erneux, G. Kozyreff, and M. Tlidi, *Phil. Trans. R. Soc. A* **368**, 483 (2010)
- [10] P. V. Paulau, D. Gomila, T. Ackemann, N. A. Loiko, and W. J. Firth, *Phys. Rev. E* **78**, 016212 (2008) Y. Tanguy, N. Radwell, T. Ackemann, and R. Jäger, *Phys. Rev. A* **78**, 023810 (2008)
- [11] M. Tlidi, A. G. Vladimirov, D. Pieroux, and D. Turaev, *Phys. Rev. Lett.* **103**, 103904 (2009)
- [12] M. Tlidi, A. G. Vladimirov, D. Turaev, G. Kozyreff, D. Pieroux, and T. Erneux, *Eur. Phys. J. D* **59**, 59 (2010)
- [13] M. Tlidi, P. Mandel, and R. Lefever, *Phys. Rev. Lett.* **73**, 640 (1994)
- [14] R. M. Corless, G. H. Gonnet, D. E. G. Hare, D. J. Jeffrey, and D. E. Knuth, *Adv. Comput. Math.* **5**, 329 (1996)
- [15] R. E. Goldstein, D. J. Muraki, and D. M. Petrich, *Phys. Rev. E* **53**, 3933 (1996)